

Fast-neutron heterogeneous scintillation detector with high discrimination of gamma background

Yuri I. Chernukhin^a, Alexei A. Yudov^{b,*}, Sergey I. Streltsov^b

^aNational Nuclear Research University “MEPhI”, 8, Komsomolskaya St., Snezhinsk, Chelyabinsk Region 456776, Russia

^bFSUE “Zababakhin All-Russia Research Institute of Technical Physics”, 13, Vasilyeva St., Shezhinsk, Chelyabinsk Region 456770, Russia

Available online 4 March 2016

Abstract

Neutron detectors have been widely used for monitoring security and illicit transportation of nuclear and radioactive materials. Distinguishing feature of such application is the necessity to measure neutron flux caused by the monitored items that is close to the natural background flux. This paper examines potential improvement of characteristics of a multi-layer neutron detector with optic fiber sensors based on lithium-silicate (⁶Li) glass, by replacing the polyethylene layers with layers of hydrogen-containing scintillating plastic. Combination of two types of neutron-sensitive sensors enables two-phase discrimination of gamma background when measured in mixed n- and gamma-fields, by the amplitude and time criteria. The proposed heterogeneous scintillation detector has much higher gamma-background discrimination factor as compared to the existing examples of multilayered neutron detectors, while maintaining rather high neutron registration efficiency, typical for multilayered detectors.

Copyright © 2016, National Research Nuclear University MEPhI (Moscow Engineering Physics Institute). Production and hosting by Elsevier B.V. This is an open access article under the CC BY-NC-ND license (<http://creativecommons.org/licenses/by-nc-nd/4.0/>).

Keywords: Heterogeneous scintillation detector; Multilayered neutron detector; Gamma-background discrimination; Optic fiber sensors based on lithium.

Neutron detectors are widely used for monitoring security and illicit transportation of nuclear and radioactive materials (NRM), which is one of the main tasks in assuring of NRM nonproliferation. Distinguishing feature of such application is the necessity to measure neutron flux caused by the monitored items that is close to the natural background flux or even less neutron (*n*) and gamma (*γ*) background fluxes whose values at the Earth’s ground level are [1–3]:

$$\begin{aligned}\varphi_{t,n} &\sim (1.1\text{--}1.5)10^{-3} \text{ n/cm}^2 \text{ s} \text{ – for thermal neutrons with energies } E_n < 0.4 \text{ eV;} \\ \varphi_{i,n} &\sim (1.9\text{--}2.9)10^{-3} \text{ n/cm}^2 \text{ s} \text{ – for intermediate neutrons with energies } E_n \sim (0.4\text{--}10^5) \text{ eV;} \\ \varphi_{f,n} &\sim (2.9\text{--}3.2)10^{-3} \text{ n/cm}^2 \text{ s} \text{ – for fast neutrons with energies } E_n \sim (0.1\text{--}10) \text{ MeV;} \\ \varphi_\gamma &\sim 5\text{--}10 \gamma/\text{cm}^2 \text{ s} \text{ – for gamma-particles with energies } E_\gamma \sim 1 \text{ MeV.}\end{aligned}$$

These data define the following requirements to fast neutron detectors applied to the above mentioned tasks:

- **High sensitivity:** To ensure the counting rate of $\sim 0.5 \text{ s}^{-1}$ for the effect comparable with the density of fast neutron flux $\varphi_e \sim \varphi_{f,n}$, the sensitivity must be $C \sim 170 \text{ cm}^2/\text{n}$.
- **High gamma discrimination ratio:** To neglect the natural gamma background while detecting fast neutrons with flux $\varphi_e \sim \varphi_{f,n}$, this ratio must satisfy $K_\gamma > 3 \cdot 10^4$; in case of additional sources of gamma background, its value must be even higher.
- **Ability to operate as a spectrometer:** To identify the monitored sources of fast neutrons and to decrease the impact of neutron background flux on to measurements in particular energy intervals.

To the most extent these requirements are satisfied by the wide-aperture, multi-layer neutron detector (MND) [4,5] developed at the Pacific Northwest National Laboratory (PNNL), USA. It is made of several layers of polyethylene with the thickness of ~ 1 to 2 cm interlaced with detecting

* Corresponding author.

E-mail address: Yudoff@mail.ru (A.A. Yudov).

Peer-review under responsibility of National Research Nuclear University MEPhI (Moscow Engineering Physics Institute).

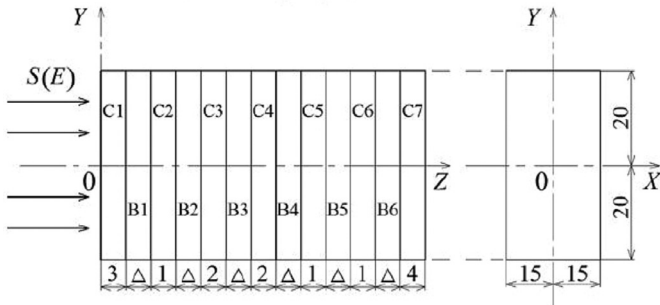


Fig. 1. Scheme of MND [6,7]: C_i , $i = 1, 2, \dots, 7$ – polyethylene layers (CH_2 , $\rho = 0.96 \text{ g/cm}^3$); B_i , $i = 1, 2, \dots, 6$ – ^6Li -activated scintillating optic fiber layers ($\text{Si}_{1.0} \text{O}_{2.58} ^6\text{Li}_{0.363} ^7\text{Li}_{0.027}$, $\rho = 2.58 \text{ g/cm}^3$, $\Delta = 0.014 \text{ cm}$); $S(E)$ – neutron (gamma) source with energy E . All sizes are given in cm.

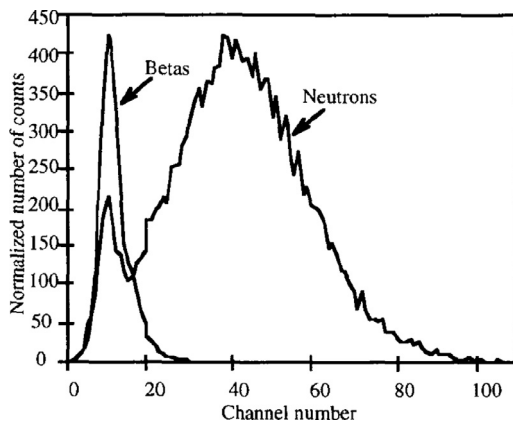


Fig. 2. Pulse-height spectra of scintillating glass fibers in neutron and beta-ray (^{90}Sr , $E_{\beta\text{max}} \sim 0.55 \text{ MeV}$) fields [8].

layers of $\Delta \sim 0.014 \text{ cm}$ effective thickness, made of cerium-activated (Ce^{3+}), lithium-silicate (with increased amount of ^6Li isotope) scintillating glass fiber (diameter $\sim 120 \mu\text{m}$) with characteristic gamma emission time of ~ 40 to 60 ns in the blue spectra range with wavelength of $\sim 470 \text{ nm}$. Fig. 1 shows scheme of the PNNL detector [6,7].

The operating principle of the detector is based on neutrons slowdown in C-layers up to thermal energies in elastic scattering by hydrogen nuclei and undergo in B-layers the exothermic $^6\text{Li}(n, \alpha)\text{T}$ reaction ($Q \sim 4.8 \text{ MeV}$), which high-energy products (T and α) induce the scintillations that are detected by photomultiplier tubes (PMT) attached to the optic fiber layers.

Investigations have shown that the total efficiency of all sensor layers to $0.5\text{--}10 \text{ MeV}$ neutrons varies in the range $300\text{--}120 \text{ cm}^2/\text{n}$. The detector is sensitive to gamma radiation as well, but due to large difference in the ranges of fast electrons, born mainly via Compton scattering of gamma particles in the detector material, as compared to the ranges of heavy charged products of the $^6\text{Li}(n, \alpha)\text{T}$ reaction taking place in the sensor layers, the amplitudes of the correspondent signals differ considerably (Fig. 2), so that discrimination of the gamma background is possible with the gamma discrimination ratio $K_\gamma \sim (1\text{--}8)10^3$ [5].

As it is noted in [7,9,10] that when signals from separate layers are detected separately, the MND can be used to assess spectral characteristics of the neutron source.

Characteristics of the MND with optic fiber sensors based on lithium-silicate (^6Li) glass shown in Fig. 1 can be improved by replacing the polyethylene layers with layers of hydrogen-containing scintillating plastic. This MND modification, referred to as heterogeneous scintillation neutron detector (HSD-n), contains two types of detectors that are sensitive to neutrons: optic fiber glass containing ^6Li and organic plastic scintillator, which makes possible to realize a multi-step discrimination of the gamma background, leading to higher values of K_γ as compared to the original MND containing only optic fiber sensors.

Numerical analysis of HSD-n has been performed with the Monte-Carlo method for the model similar to that shown in Fig. 1, except layers C_i ($i = 1, 2, \dots, 6$) were filled with polystyrene scintillator ($\text{CH}_{1.1}$, $\rho = 1.06 \text{ g/cm}^3$), $S(E)$ is a planar homogeneous monodirectional source of neutrons and photons with energy E . The sum of signals in all B_i ($i = 1, 2, \dots, 6$) and C_i ($i = 1, 2, \dots, 6$) layers is calculated. Results are normed per one source particle (neutron or photon). The following values have been calculated:

- The rate of $^6\text{Li}(n, \alpha)\text{T}$ reaction in the B layers for source neutrons with energy $E_n = 0.1\text{--}0.8 \text{ MeV}$, which describes the detecting efficiency of these neutrons in B layers, $\epsilon_n^B(E_n)$
- Time dependence of this value for a prompt $1\text{--}8 \text{ MeV}$ neutron source, normalized to its maximal value,

$$W_n^B(t, E_n) = \epsilon_n^B(t, E_n) / \epsilon_n^B(E_n) \quad (1)$$

- Energy spectrum of the neutron fluence $\Phi(E)$ in C layers, and the correspondent spectrum of recoil protons that arise in elastic scattering by hydrogen nuclei, for source neutrons with energy $E_n = 0.7\text{--}8 \text{ MeV}$

$$R(E_p, E_n) = \sum_{i=1}^6 V_i \int_0^{E_n} \Sigma_H(E') \frac{1}{E'} [\eta(E_p) - \eta(E_p - E')] \times \Phi_i(E') dE' = \sum_{i=1}^6 V_i \int_{E_p}^{E_n} \Sigma_H(E') \frac{\Phi_i(E')}{E'} dE' \quad (2)$$

and the source neutron detecting efficiency taking into account the recoil-protons detecting threshold $E_{p,t} = 0.5 \text{ MeV}$ in C channels,

$$\epsilon_n^C(E_n) = \int_{E_{p,t}}^{E_n} R(E_p, E_n) dE_p, \quad (3)$$

where $\Sigma_H(E')$ is the elastic scattering macroscopic cross-section of neutrons with energy E' on hydrogen nuclei, V_i – volume of layer C_i , $\eta(E')$ – the Heaviside step function and $E_{p,n}$ – the proton detection threshold.

- For photon source with energy $E_\gamma = 0.5\text{--}10 \text{ MeV}$, probability distribution $W_\gamma^B(\varepsilon)$ of energy ε absorbed in B layers,

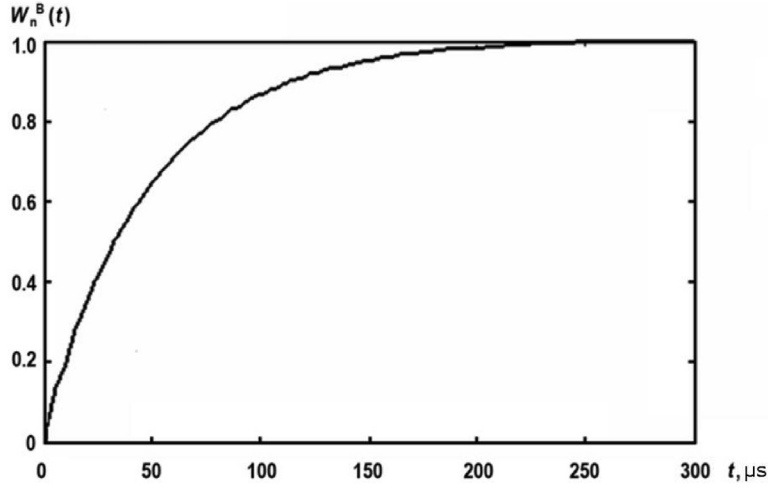


Fig. 3. Detecting efficiency time dependence of 1–8 MeV neutrons in B channels of HSD-n.

Table 1
Probability density of photon energy absorption in B layers of HSD-n.

E_γ , MeV	W_γ^B , 10^{-2} 1/MeV				
$\Delta\epsilon$, MeV	0.5	1.0	2.0	4.0	10
0.1–0.25	6.20	9.13	12.3	17.2	31.9
0.25–0.5	0.32	1.28	2.16	2.92	4.56
0.5–0.75	0	0.024	0.16	0.36	0.68
0.75–1.0	0	0	0.008	0.04	0.08
1.0–1.5	0	0	0	0.002	0.016
>1.5	0	0	0	0	0

and the correspondent detecting efficiency of these photons in B layers for two values of the detecting energy threshold, $\epsilon_{t1}=0.25$ MeV and $\epsilon_{t2}=0.5$ MeV:

$$\epsilon_\gamma^B(E_\gamma, \epsilon_t) = \int_{\epsilon_t}^{E_\gamma} W_\gamma^B(\epsilon, E_\gamma) d\epsilon \quad (4)$$

It was assumed that recoil protons with energies $E_p \geq E_{p,t}$ in C layers, energy losses of photons with $\epsilon \geq \epsilon_t$, and reactions ${}^6\text{Li}(n, \alpha)\text{T}$ in B layers are detected with 100% probability.

Main calculation results are presented in Tables 1–3 and in Fig. 3. According to Table 1, the maximal absorbed energy in B layers for a wide source gamma energy range $E_\gamma \approx 1$ –10 MeV does not exceed $\epsilon_m \sim 1.5$ MeV, which is below the energy of charged products of ${}^6\text{Li}(n, \alpha)\text{T}$ reaction that defines neutron detection in these layers,

$$\epsilon_m \ll Q \sim 4.8 \text{ MeV} \quad (5)$$

This relation can be used to significantly reduce the photon detecting efficiency in the B-channels, by choosing a proper value of the threshold energy ϵ_t , without deteriorating the neutron detection efficiency in the same channel. According to the data in Table 2, the gamma discrimination ratio of the ~ 2 MeV gamma rays in the B-channel at $\epsilon_t = 0.5$ MeV amounts to $K_\gamma = 2.5 \cdot 10^3$. This value grows as energy E_γ decreases.

Table 2
Photon detecting efficiency in B layers of HSD-n.

E_γ , MeV	ϵ_γ^B , %				
ϵ_t , MeV	0.5	1.0	2.0	4.0	10
0.25	0.08	0.33	0.58	0.83	1.34
0.5	0	0.006	0.04	0.10	0.20

As analysis has shown, relation (5) is due to the fact that scintillation in the B-channels (that are $\Delta = 0.014$ cm thick in the HSD-n design) is caused mainly by fast electrons, generated in more thick (~ 1 cm) C-channels. This means that detection of both neutrons and gamma particles in the B layers of HSD-n is a secondary process with respect to their primary interaction in the C layers, that is, each detection event in a B layer is preceded by a neutron- or gamma induced event in a C layer. For gamma responses, the time interval between these two events, τ^{CB} , is assessed to be smaller than 10 ns.

The fast neutrons detection time interval, τ_n^{CB} , has been found from the dependency $W_n^B(t)$, calculated for the considered HSD-n design for source neutron energies in the range $E_n = 1$ –8 MeV, shown in Fig. 3. In this time interval, this dependence is practically independent on the energy E_n , and can be approximated with 5% accuracy by the function

$$W_n^B(t) = 1 - \exp(-t/t_0), \quad t_0 = 46.3 \mu\text{s} \quad (6)$$

This function gives $\tau_n^{CB} = 200 \mu\text{s}$ that exceeds considerably $\tau_{\gamma \max}^{CB}$:

$$\tau_n^{CB} \gg \tau_{\gamma \max}^{CB} \quad (7)$$

that is governed by the processes of neutron slowing down and thermalization in the C layers.

Relation (7) gives possibility to discriminate gamma background by the time criterion in the neutron measurements with the help of HSD-n. For this to achieve, the detection scheme must be equipped with the output signals from B- and C layers coincidence circuit in a “detection window” appropriately set to $\Delta\tau_{CC} \approx 0.1$ –200 μs according to Fig. 3. This choice

Table 3
Neutron detecting efficiency in B and C layers of HSD-n.

E_n , MeV	0.1	0.7	1.0	2.0	4.0	6.0	8.0
ϵ_n^B , %	21.8	22.3	21.4	17.9	12.6	10.2	7.9
ϵ_n^C , % ($E_{p,t}=0.5$ MeV)	–	24.6	51.0	86.5	94.1	84.1	75.5

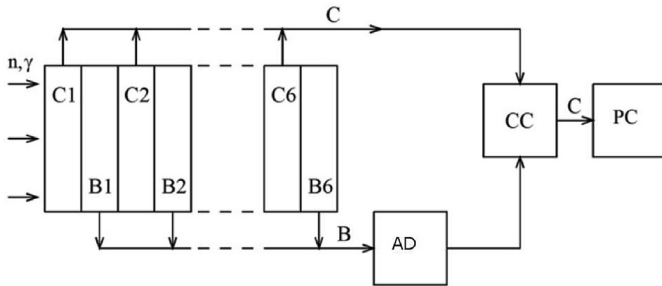


Fig. 4. HSD-n signal registration scheme with two phases of gamma discrimination: C – channel for the C layers (made of scintillating plastic); B – channel for the B layers (^6Li -containing glass fiber); AD – amplitude discriminator; CC – coincidence circuit; and PC – counter.

assures the fast-neutron detection efficiency close to its maximal achievable value and practically complete discrimination of gamma particles when measuring in the mixed neutron and gamma fields. Calculated values of detection efficiencies ϵ_n^B and ϵ_n^C in the B- and C-HSD-n measurement channels are presented in Table 3, from which it follows that the detector efficiency in the “coincidence” operation mode will be close to ϵ_n^B that amounts to 10% for energies $E_n \sim 1\text{--}8$ MeV.

A signal registration scheme of HSD-n with two phases of gamma discrimination is shown in Fig. 4. When registering fast neutrons, AD in the B channel passes signals having the amplitude above A_0 that corresponds to neutron signals, and blocks signals having the amplitude $A < A_0$ corresponding to gamma signals (the first n-, gamma discrimination phase, according to criterion (5)). Signals that were passed through the B-channel discriminator (that are secondary with respect to the signals in channel C), together with the C-channel signals (primary) are received by the coincident circuit CC with “detection window” $\Delta\tau_{CC}$, and passed to the counter PC if $\tau^{CB} \in \Delta\tau_{CC}$, i.e. when signals are identified as coming from neutrons (the second phase of n-, gamma discrimination, according to criterion (7)).

The HSD-n measuring scheme (Fig. 4) can operate as a spectrometer with high gamma discrimination. To achieve this, the counter PC must be replaced with an impulse amplitude analyzer for the C-channel signals, measuring recoil-proton energy spectrum $F(E_p)$ in the C layers of the detector. In this case, the energy distribution of neutron fluence $\Phi(E)$ at the detector input aperture is defined by the following relation:

$$F(E_p) = P \cdot \int_{E_i}^{E_m} R(E_p, E) \cdot \Phi(E) dE \quad (8)$$

where $R(E_p, E)$ is the response function of the C-channel spectrometer, normalized to one source neutron, E_m – is the neutron source maximal energy.

One of the drawbacks of the considered HSD-n measuring scheme is that it operates only in a single-particle detection mode, which considerably limits its maximal loading. This drawback can however be eliminated by applying in the C layers newly developed plastic scintillators featuring n-, gamma discrimination by the fluorescence impulse time shape [11]. The use of such scintillators in the C layers of HSD-n improves the response time, as well as introduces a third phase of gamma background discrimination by the signal pulse shape detected in the C-channel.

Conclusion

Operation of the fast-neutron heterogeneous scintillating detector (HSD-n) consisting of paired layers of 1–2 cm thick polystyrene scintillators (C layers) and scintillating optic fiber (B layers) having the effective thickness of ~ 0.014 cm made of lithium-silicate (^6Li) glass is analyzed.

This combination of sensitive to neutrons detectors makes possible to organize the two-phase discrimination of gamma background when performing measurements in mixed n- and gamma fields: by the amplitude criterion (due to the discrepancy of signal amplitudes coming from neutrons and gamma particles in the B-channel) and by the time criterion (due to large difference in time intervals τ^{CB} between the correlated signals in the C- and B-channels induced by neutrons and gamma particles).

It is shown that with the quantitative values describing the above mentioned criteria chosen in this work, the detecting scheme of HSD-n features much higher gamma-background discrimination coefficient, as compared to the MND with C-layers made of polyethylene [5,7], while still keeping a comparatively high efficiency of neutron detection, specific to MND.

It is noted that the parameters of the HSD-n measuring scheme can be considerably improved by replacing the polystyrene scintillators in the C layers with newly-developed plastic scintillators that feature n-, gamma discrimination by the fluorescence pulse shape.

References

- [1] V.V. Vladislavlev, At. the. rub. 3 (1992) 2225 (in Russian).
- [2] V.V. Frolov, Yaderno fizicheskie metody kontrolya delyaschikhsya veschestv [Nuclear-physics methods of controlling fissionable materials], Energoatomizdat Publ, Moscow, 1989 in Russian.
- [3] A.A. Moiseev, V.I. Ivanov, Spravochnik po dozimetrii i radiatsionnoj gigiene [Handbook on dosimetry and radiation hygiene], Energoatomizdat Publ, Moscow, 1990 in Russian.
- [4] M. Bliss, P.L. Reder, R.A. Craig, in: Paper on Institute of Nuclear Materials Management Annual Meeting, 17–20 July, Naples, FL, US, 1994.
- [5] R.S. Seymour, M. Bliss, B. Richardson, C.D. Hull, D.S. Barnett, Proceedings of SPIE: Volume 3536. Nuclear Waste Instrumentation Engineering, Global Trade Media, 29 January, 1999. <http://spie.org/Publications/Proceedings/Paper/10.1117/12.339067>
- [6] Craig R.A., Bliss M. Predicted performance of neutron spectrometers using scintillating fibers. http://www.pnl.gov/main/publications/external/technical_reports/PNNL-13111.pdf, 2010 (accessed 10.04.10).

- [7] M. Bliss, R.A. Craig, D.S. Barnett, D.N. Anderson, J.E. Smart, M.A. Knopf, S.A. Hartley, in: Paper on Annual Meeting of the Institute of Nuclear Materials Management, 15–19 July, Indian Wells, CA (US), 2001.
- [8] M. Bliss, R.A. Craig, P.L. Reeder, D.S. Sunberg, IEEE Trans. Nucl. Sci. 42 (1995) 639–643.
- [9] M. Bliss, R.A. Craig, D.S. Sunberg, in: Proceedings of Third Pacific Northwest Fiber Optic Sensor Workshop, 2 September, Vol. 3180, SPIE Proceedings Series, PNNL, 1997.
- [10] G.L. Dedenko, V.V. Kadilin, S.V. Kolesnikov, V.T. Samosadnyi, Atomic Energy 99 (2) (2005) 141–147.
- [11] N. Zaitseva, L. Carman, A. Glenn, I. Pawelczak, P. Martinez, S. Hamel, B. Rupert, N. Cherepy, S. Payne, Paper on VNIIA US-Russian Workshop on Radiation Detection, 23–27 January, 2012.